Optics Communications 283 (2010) 1869–1872

Contents lists available at ScienceDirect

Optics Communications

journal homepage: www.elsevier.com/locate/optcom

Ultrafast temperature relaxation evolution in Au film under femtosecond laser pulses irradiation

Guangqing Du, Feng Chen *, Qing Yang, Jinhai Si, Xun Hou

Key Laboratory for Physical Electronics and Devices of the Ministry of Education and Key Laboratory of Photonics Technology for Information, Shaanxi Province, School of Electronics and Information Engineering, Xi'an Jiaotong University, No. 28, Xianning West Road, Xi'an 710049, PR China

ARTICLE INFO

Article history:
Received 16 November 2009
Received in revised form 15 December 2009
Accepted 16 December 2009

Keywords:
Femtosecond laser pulses
Two temperature model (TTM)
Fourier thermal diffusion
Relaxation time

ABSTRACT

Ultrafast temperature relaxation processes in Au film including two temperature relaxation and thermal diffusion relaxation with femtosecond laser pulse excitation were investigated numerically by Finite Element Method (FEM). With the temperature dependent thermal parameters, the full 2D temperature field evolution in picosecond and nanosecond domains were obtained. It is proposed that the heat transfer depth can be alternatively localized or enhanced by the distinct temperature relaxation mechanisms. Moreover, the effect of laser parameters and Au film thickness and surface reflectivity on the two temperature relaxation time were analysed.

1. Introduction

With recent progress of laser systems, especially those based on the Chirped Pulse Amplification (CPA) technique, the laser pulse duration can be varied from several nanoseconds to about a few femtoseconds (10^{-15} s) and the intensity can even be up to 10^{21} W/m^2. The inherent characteristics of femtosecond laser pulses such as high peak power, short pulse duration and optional pulse train output can bring in the available advantages of a low ablation threshold, ultrahigh precision, minimal collateral thermal damage and large material removal rate in femtosecond laser material processing [1–6]. For pulsed laser ablation of metals, the energy relaxation mechanisms perform great disparity for femtosecond and nanosecond pulse duration. In fact, the electron and phonon relax synchronously for the nanosecond laser ablation, however, which are out of equilibrium severely for femtosecond laser ablation due to the femtosecond pulse duration is quite shorter compared to the electron–phonon relaxation time [7–12].

The dominant mechanisms for femtosecond laser pulses interaction with metals consist of three stages. The first stage is the absorption of the laser energy through photon–electron coupling within the femtosecond pulse duration. It takes a few femtoseconds for electrons to reestablish the Fermi distribution meanwhile the metal lattice keep undisturbed. The second stage is the energy distribution to the lattice through electron–phonon coupling, typically on the order of tens of picoseconds. The last stage is the normal energy diffusion into the bulk through phonon–phonon collisions, which will dominate the main heat transfer process after termination of the electron–phonon coupling process.

It is believed that the electron–phonon coupling, also called two temperature relaxation play an important role in processing of metallic targets under ultrashort laser pulses irradiation in the ablation regime [13]. However, the two temperature relaxation strength varies significantly for different metals and can be influenced by different irradiation conditions [14,15]. Furusawa et al. analytically investigated the effect of laser pulse duration on the two temperature relaxation time [16]. Chen et al. presented a temperature dependent electron–phonon coupling strength expression that can educe the temperature dependent two temperature relaxation time [17]. Even so, because of the requirements on fabrication of super precision functional devices such as photo mask and integrated optical circuit with the ultrashort pulses laser, the investigation of more influencing factors for the two temperature relaxation process are actually urgent for optimal processing of target material. To our knowledge, a more detailed insight into the full temperature relaxation processes and the effect such as laser fluence and film thickness and reflectivity on the two temperature relaxation are less theoretically investigated so far.

In this letter, we numerically investigated two sequential temperature relaxation processes in Au film target exposed to single femtosecond laser pulse. The simulated 2D full temperature field evolution pictures for the two distinct relaxation processes are obtained with the finite element method (FEM). The temperature dependent thermal parameters for Au target are taken in account and the ballistic effect is also included in our calculation. The effect

* Corresponding author. Tel./fax: +86 029 82665105.
E-mail address: chenfeng@mail.xjtu.edu.cn (F. Chen).

0030-4018/$ - see front matter © 2009 Elsevier B.V. All rights reserved.
doi:10.1016/j.optcom.2009.12.038

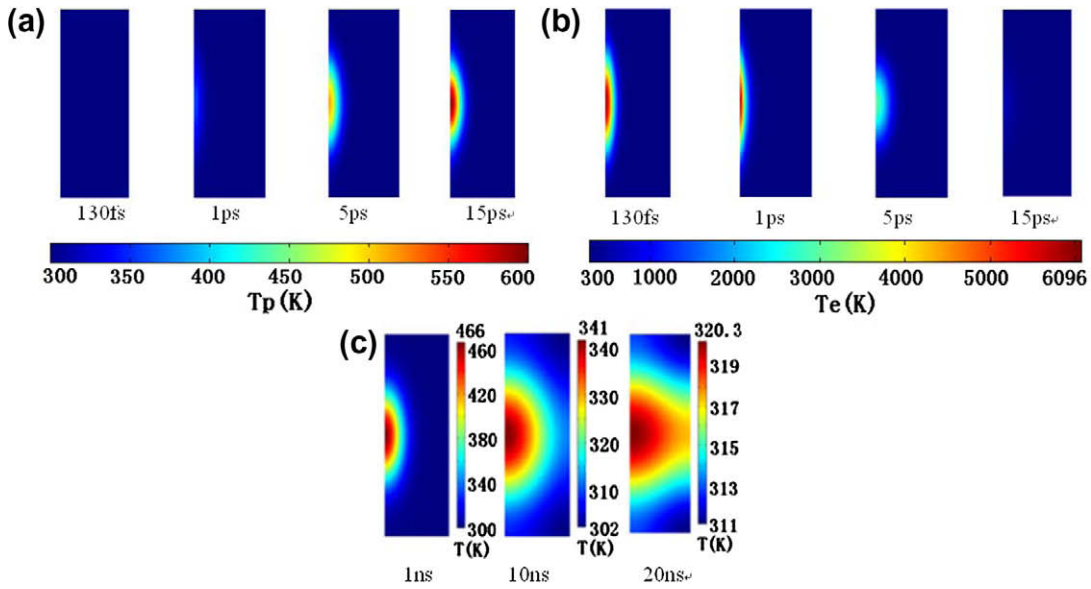

Fig. 1. 2D temperature field distributions at different time: (a) phonon temperature fields, (b) electron temperature fields, and (c) united electron–phonon temperature fields.

of laser parameters and Au film thickness and surface reflectivity on the two temperature relaxation time are carefully analysed, the results provide the theoretical guidance for optimal processing of Au film, more generally the metallic targets under the ultrashort pulses laser irradiation.

2. Modeling and discussion

The well-known two temperature model (TTM) which is originally proposed by Anisimov et al. is as follows [18]:

$$C_e\frac{\partial T_e}{\partial t}=\nabla(k_e\nabla T_e)-g(T_e-T_p)+Q, \tag{1}$$

$$C_p\frac{\partial T_p}{\partial t}=g(T_e-T_p), \tag{2}$$

where the subscripts e and p refer to the electron and phonon parameters; $C_e=C_{e0}(T_e/T_0)$ and $k_e=k_0(T_e/T_p)$ is the temperature dependent heat capacity and heat conductivity, respectively; C_P is the phonon thermal capacity which can be considered as a constant; and g is the electron–phonon coupling strength. The phonon heat conduction is neglected due to the phonon diffusion time is quite longer compared to two temperature relaxation time. The 2D energy absorption rate Q is

$$Q=S(x,y)\cdot T(t), \tag{3}$$

where

$$S(x,y)=\sqrt{\frac{4\ln 2}{\pi}}\frac{1-R}{t_p(\delta+\delta_b)}F\times\exp\left[-\frac{x}{\delta+\delta_b}-\left(\frac{y-y_0}{y_s}\right)^2\right], \tag{4}$$

$$T(t)=\exp\left(-4\ln 2\left(\frac{t-2t_p}{t_p}\right)^2\right), \tag{5}$$

Here, R is the Au film surface reflectivity, t_p is the FWHM (full width at half maximum) pulse duration, $\delta=15.3$ nm the optical penetration depth, and $\delta_b=100$ nm the ballistic length for Au film. F is the laser fluence, which can be taken as optional values in our simulation. y_0 is the coordinate of the central spot of light front at the plane of incidence and y_s is the profile parameter.

Because of the flexibility of finite element method in dealing with heat transfer equations, the partial differential Eqs. (1) and (2) are simultaneously solved by the FEM. The calculation starts at time $t=0$. The initial conditions for both electrons and phonons are assumed to be room temperature. Thus

$$T_e(x,y,0)=T_p(x,y,0)=300\ \text{K}. \tag{6}$$

During the femtosecond-to-picosecond time period, it is reasonable to assume that heat losses from the metal film to the surrounding as well as to the front surface are neglected, and the perfect thermal insulation between Au film with substrate is assumed at the rear surface. Therefore, the boundary conditions can be written as

$$\partial T_e/\partial n|_\Omega=\partial T_p/\partial n|_\Omega=0. \tag{7}$$

Here, Ω represents the four borderlines of the 2D Au film. The film thickness and width are taken as 3 μm and 8 μm, respectively. The other parameters are listed as follows:

$k_0=315\ \text{W/(mK)}$, $C_{e0}=2.1\times10^4\ \text{J/(m}^3\text{K)}$, $C_p=2.5\times10^6\text{J/(m}^3\text{K)}$,
$g=2.6\times10^{16}\ \text{W/(m}^3\text{K)}$,
$y_s=1.5\ \mu\text{m}$, $y_0=4\ \mu\text{m}$, $R=0.93$,
$t_p=65\ \text{fs}$, $F=0.5\ \text{J/cm}^2$.

The simulated results of the 2D temperature relaxation evolution pictures are shown in Fig. 1. It can be seen from Fig. 1a and b that at time 130 fs, the phonons keep cool, whose temperature is close to the initial room temperature 300 K. In contrast, the electrons are overheated, the temperature of electrons at the front surface is 6096 K. The temperature difference between phonons subsystem and electrons subsystem is very remarkable, it is indicated that the electrons and phonons are out of equilibrium drastically at this time. After 130 fs, the phonons temperature begins to rise and reaches to 360 K at 1 ps at the front surface of Au film, meanwhile, the electron temperature at the front surface of Au film drops to 5848 K. At time 5 ps, the tendency of electrons temperature drop and phonons temperature rise becomes more obviously, and the maximal temperature for phonons and electrons at the front surface is 515.2 K and 2979 K, respectively. We notice that the phonons and electrons temperature fields penetrate into deeper inner region at this time, which shows the electrons heat diffusion dominates the evolution during this period.

At time 15 ps, the phonons and electrons temperature fields form uniform distribution, with temperature of 600 K on the laser irradiated surface. After 15 ps, the calculation shows that the

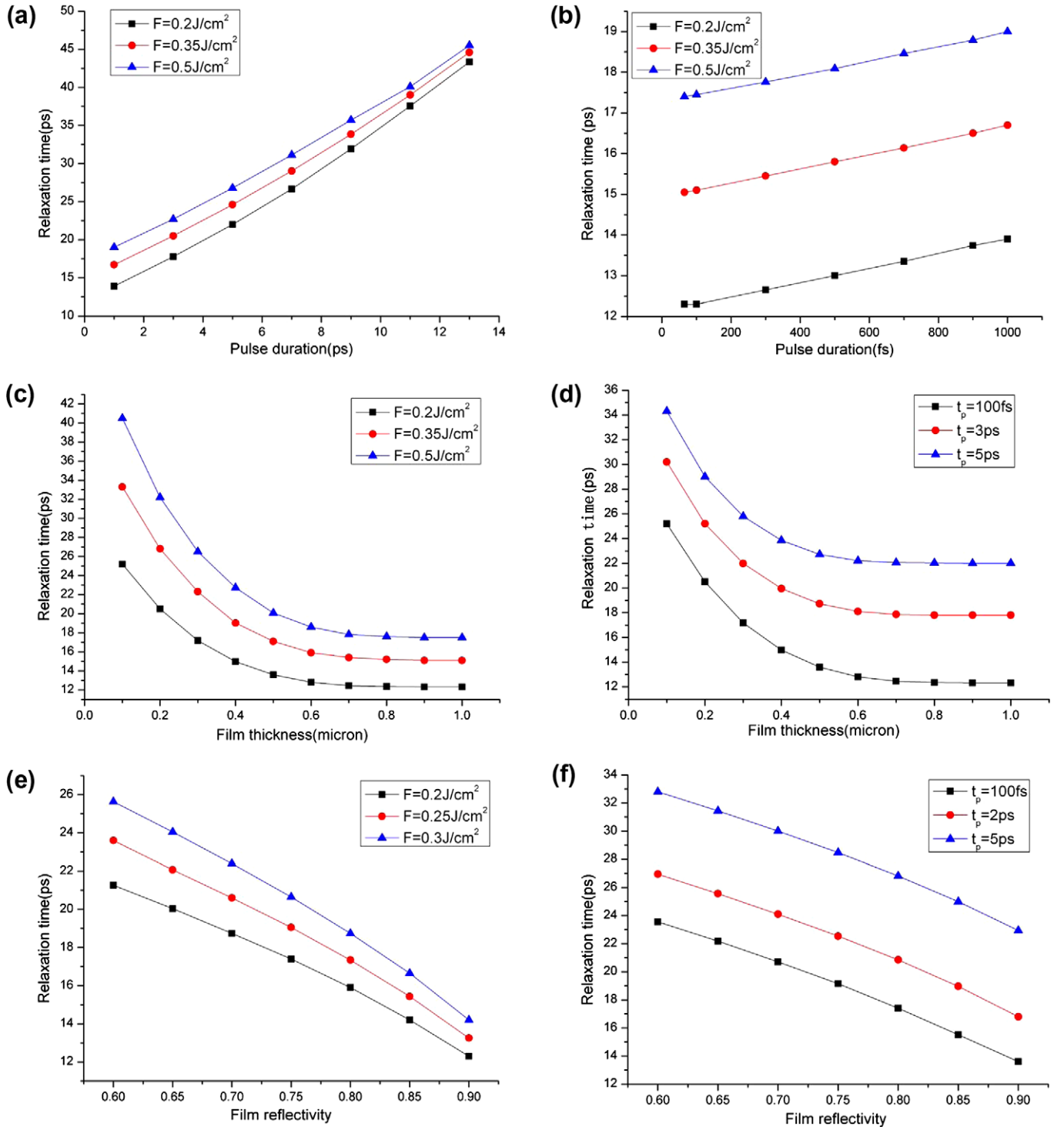

Fig. 2. The dependence of two temperature relaxation time on laser duration, film thickness and reflectivity: (a) reflectivity $R = 0.90$, film thickness $d = 3$ μm, (b) reflectivity $R = 0.90$, film thickness $d = 3$ μm (c) reflectivity $R = 0.90$, pulse duration $t_p = 100$ fs, (d) reflectivity $R = 0.90$, laser fluence $F = 0.20$ J/cm², (e) film thickness $d = 3$ μm, pulse duration $t_p = 65$ fs, and (f) film thickness $d = 3$ μm, laser fluence $F = 0.25$ J/cm².

temperature field is severely restrained and localized. In fact, however, after 15 ps the temperature fields of electrons and phonons evolve simultaneously, the temperature relaxation is mainly dominated by the thermal diffusion mechanism which is represented by the following normal Fourier thermal diffusion equation:

$$C\frac{\partial T}{\partial t} = \nabla(k\nabla T) - \varepsilon\sigma(T^4 - T_0^4)d^{-1}, \tag{8}$$

where C is the heat capacity of Au in the electron–phonon equilibrium state, k is the heat conduction

$$k = 320.973 - 0.0111 \times T - 2.747 \times 10^{-5} \times T^2 - 4.048 \times 10^{-9} \times T^3, \tag{9}$$

ε is the emissivity taken as 0.03, σ is the Stefan–Boltzmann constant, d is the film thickness and T_0 is the ambient air temperature taken as 300 K in room temperature. The last term in Eq. (8) represents the radiation heat loss to the ambient environment, which could also be considered as the boundary condition, nevertheless the heat loss to ambient environment is smaller in our simulation

due to the slight temperature difference between Au surface and the ambient air.

The thermal diffusion equation is solved following the two temperature relaxation termination at 15 ps. Fig. 1c shows the simulated results of 2D equilibrium temperature field evolution pictures at three different time points in nanosecond domain. At time 1 ns, the maximal temperature at front surface is 466 K, which is quite lower compared to the electron–phonon equilibrium temperature 600 K at 15 ps, and the temperature field penetration is significantly enhanced at this time. At time 10 ns, the temperature field continues to penetrate into the inside region of the Au film, the maximal temperature at the front surface and rear surface become 341 K and 314 K, respectively. At time 20 ns, the front surface temperature of the Au target decrease to 320.3 K and the rear surface temperature increase to 317 K. In this way, the Au target cool down and ultimately the energy in the Au film gets thermal equilibrium with ambient air.

When the laser energy is high enough, the melting time of metal lattice is less than the two temperature relaxation time, so the equilibrium heat diffusion relaxation can be omitted safely because the target material has been removed at the termination of two temperature relaxation process, the deposited heat energy is mainly taken away by the vapor and plasma plume. It is implied that the two temperature relaxation which is responsible for metal ablation at high laser intensity regime, plays a key role in ultrashort pulse ablation of metallic films.

In light of the importance of the two temperature relaxation, and it's easily subjected to external factors such as laser parameters and material characteristic. In the following, we focus on investigating the effect of pulse duration, target thickness and reflectivity on the two temperature relaxation time. The TTM equations are solved using the FEM considering varying parameters like laser fluence, pulse duration, metallic reflectivity and film thickness, respectively. The initial and boundary conditions are referred before. The simulated results are shown as Fig. 2. We can see from Fig. 2a that for different laser fluences, the two temperature relaxation time increase dramatically with increase of pulse duration in picosecond time domain. However, in femtosecond time domain as shown in Fig. 2b, there is a slight increase of two temperature relaxation time with pulse duration. In Fig. 2c, it is shown that the two temperature relaxation time decrease dramatically with increase of Au film thickness when the thickness is less than 0.6 μm, once the thickness exceeds 0.6 μm, the two temperature relaxation time keep constants with values of 12.3 ps, 15.1 ps and 17.4 ps for three different laser fluences of 0.2 J/cm^2, 0.35 J/cm^2 and 0.5 J/cm^2, respectively. In addition, the simulation shows the calculated critical film thickness 0.6 μm is conformable for the laser threshold fluence. Considering the linear relationship between laser threshold fluence and the two temperature relaxation time under the assumption of constant thermal diffusion velocity [19]. So we reasonably conclude that the threshold fluence is also not affected by the film thickness when it is larger than 0.6 μm, which is further validated by the published works [13]. It also been proved by our simulation can be seen from Fig. 2d that for different pulse durations of 100 fs, 3 ps and 5 ps, when the thickness is larger than 0.6 μm, the two temperature relaxation time is also immune to the film thickness. Figs. 2e and f show that the two temperature relaxation time decrease with increasing the surface reflectivity for different laser fluences and durations, respectively. It can be explained as follows: the high reflectivity can cut down the incidence laser energy into the metallic film, whereas, the lower energy results in the smaller two temperature relaxation time, so a more smooth metal surface, namely the surface with high reflectivity, leads to the smaller two temperature relaxation time. It is also suggested that appropriate roughening of the metallic target surface can result in the increase of the two temperature relaxation time, which is beneficial for enhancing the heat penetration into the inner region of the target material.

3. Conclusion

In this paper, we numerically investigated the ultrafast temperature relaxation processes including two temperature relaxation and thermal diffusion relaxation. The results showed that the two temperature relaxation can lead to the localization of the energy deposition. However, the thermal diffusion relaxation will make the energy penetrating into deeper region of the target material. It is revealed that the effect of picosecond laser pulse on the two temperature relaxation time is more violent than that of the femtosecond laser pulse, and the two temperature relaxation time is immune to the Au film thickness when it is larger than 600 nm. Moreover, a rough metallic surface can result in a larger two temperature relaxation time, which is beneficial for heat penetrating into the inner region of the target.

Acknowledgement

The work was supported by National High Technology R&D Program of China under the Grant No. 2009AA04Z305 and National Science Foundation of China under the Grant Nos. 60678011 and 10674107.

References

[1] Godai Miyaji, Kenzo Miyazaki, Opt. Express 16 (2008) 16265.
[2] P.P. Pronko, S.K. Dutta, J. Squier, J.V. Rudd, D. Du, G. Mourou, Opt. Commun. 114 (1995) 106.
[3] X. Liu, D. Du, G. Mourou, IEEE J. Quant. Electron 33 (1997) 1706.
[4] Jörg Krüger, Daniela Dufft, Robert Koter, Andreas Hertwing, Appl. Surf. Sci. 253 (2007).
[5] J. Bonse, J.M. Wrobel, J. Krüger, W. Kautek, Appl. Phys. A 72 (2001) 89.
[6] S. Preuss, A. Demchuk, M. Stuke, Appl. Phys. A61 (1995) 33.
[7] B.N. Chichkov, C. Momma, S. Nolte, F. von Alvensleben, A. Tünnermann, Appl. Phys. A63 (1996) 109.
[8] J.K. Chen, W.P. Latham, J.E. Beraun, Numer. Heat Transfer B: Fundam. 42 (2002) 1.
[9] J.K. Chen, J E Beraun, J. Opt. A: Pure Appl. Opt. 5 (2003) 168.
[10] A.P. Kanavin, I.V. Smetanin, V.A. Isakov, Yu.V. Afanasiev, Phys. Rev. B 57 (1998) 698.
[11] M.I. Kaganov, I.M. Lifshitz, M.V. Tanatarov, Sov. Phys. JETP 4 (1957) 173.
[12] R.W. Schoenlein, W.Z. Lin, J.G. Fujimoto, Phys. Rev. Lett. 58 (1987) 1680.
[13] S.-S. Wellershoff, J. Hohlfeld, J. Güdde, E. Matthias, Appl. Phys. A 69 (Suppl.) (1999) 99.
[14] M.A. Al-Nimr, V.S. Arpaci, J. Appl. Phys. 85 (1999) 2517.
[15] D.Y.T. Zou, J.K. Chen, J. E Beraun, Int. J. Heat Mass Transfer 45 (2002) 3369.
[16] K. Furusawa, K. Takahashi, H. Kumagai, K. Midorikawa, M. Obara, Appl. Phys. 69A (Suppl.) (1999) 359.
[17] J.K. Chen, W.P. Latham, J.E. Beraun, J. Laser Appl. 17 (2005) 63.
[18] S.I. Anisimov, B.L. Kapeliovich, T.L. Perel'man, Sov. Phys. JETP 39 (1974) 375.
[19] P.B. Corkum, F. Brunel, N.K. Sherman, Phys. Rev. Lett. 61 (1988) 2886.